
**AIRCRAFT INSTRUMENTS
AND INSTRUMENTATION COMPUTER COMPLEXES**

Method for Equipping the Aircraft Gas Turbine Engine with Vibration Sensors by Evaluating Their Information Content Based on Mathematical Modeling

K. V. Shaposhnikov^{a,*}, A. V. Davydov^a, S. A. Degtyarev^a, M. K. Leont'ev^a, and I. L. Gladkii^b

^a*Alfa-Tranzit Co., Ltd., ul. Leningradskaya 1, Khimki, Moscow oblast, 141400 Russia*

^b*UEC Aviadvigatel JSC, pr. Komsomol'skii 93, Perm, 614920 Russia*

**e-mail: kvshaposhnikov@alfatran.com*

Received October 4, 2022; revised October 15, 2022; accepted October 15, 2022

Abstract—The paper proposes a novel method for determining the location of vibration sensors on the aircraft engine case in order to enhance their information content by mathematical modeling. The method is based on calculation of the engine critical speeds and analysis of their vibration mode shapes using the general dynamic model of the engine. The method was tested on the engine model and allowed forming the installation scheme of sensors with high information response on vibration excitation generated by its rotors.

DOI: 10.3103/S1068799822040225

Keywords: aircraft engine, vibration sensors, rotor dynamics, scheme of vibration sensors installation, critical speed, rotor–case–suspension, modeling, DYNAMICS R4.

INTRODUCTION

Modern aircraft engines are complex dynamic systems, which include a large number of interacting elements and subsystems. Numerical models developed by engineers for evaluation of engine dynamics in operation are also complicated. Verification of such models includes control of mass and inertia properties for engine parts and assemblies for compliance with their actual values as well as numerical reproduction of all critical speeds that are allowed by design engineers in operating range of the engine. At the same time, there is a keen problem for identification of all engine critical speeds. International standards for model creation for rotor dynamics simulation impose strict requirements on verification of numerical models: deviation between critical speeds obtained experimentally and numerically should not exceed 5% [1]. In domestic aircraft engine manufacturing, there are no standards similar to API [1] with such detailed requirements for rotor dynamics models, therefore, aircraft engine manufacturers often evaluate accuracy of their numerical models in accordance with enterprise practice for such model creation when verifying reproduction of the position of critical speeds and their amplitudes [2].

Sensors used for evaluation of engine overall vibration in operation are called permanent. Vibration at the permanent sensor locations not necessarily should be maximum, but essentially most typical, clear and steadily connected with excitation forces [3]. Since permanent sensors are usually located at suspension mounts and register vibration only in one or two directions (radial and axial, or just radial), then frequently it is not possible to identify all critical speeds of the engine based on their measurements because due to dynamic system orthotropy, critical speed mode shapes may have significant displacements at directions that are not controlled by permanent sensors. Vibration amplitude of permanent sensors can also be small and free from obvious vibration peaks, creating significant difficulties for clear identification of certain critical speeds. Thus, design engineers often face a difficult

task having to equip an aircraft engine with additional vibration sensors for verification of its numerical model and to conduct additional special experiments.

In practice of domestic aircraft engine manufacturing, selection of vibration sensors scheme is usually determined by the diagnostics task and prior knowledge about vibration dynamics of predecessor engines. When a diagnostics task is not clear and prior information is scarce, e.g., during new engines development, a greater number of points and object parameters are subjected to examination and a more detailed analysis of vibration signals and their characteristics is required for diagnostics [4].

MODEL OF AIRCRAFT ENGINE DYNAMIC SYSTEM

The tendency for maximum engine weight reduction leads to usage of lightweight cases and rotors in structure schemes of modern aircraft engines. In certain instances, natural frequencies of the engine cases can be lower than bending natural frequencies of its rotors. In this case, vibration dynamics of engines individual subsystems could not be considered separately from the whole engine dynamic system [3]. Hence, dynamic scheme of the engine should be considered as a uniform “rotor–case–suspension” dynamic system. Problems of such systems modeling were described in detail in works of Natanzon V.Ya [5], Krukov K.A. [6], Gurov A.F. [7], Hronin D.V. [8], Ivanov A.V. [9], Potapova O.Yu. [10], Novikov D.K. [11], Zrelov V.A. [12], Nikhamkin M.Sh. [14], Leont’ev M.K. [14]. Detailed review of various methods for turbomachinery rotor–case dynamic system modeling could be found in [15].

The method of model creation for rotor dynamics simulation is based on representation of engine dynamic system in form of a discrete finite element model consisting of subsystems [16]. Model of a high-bypass turbofan engine built in software for rotor dynamics simulation DYNAMICS R4 is shown in Fig. 1.

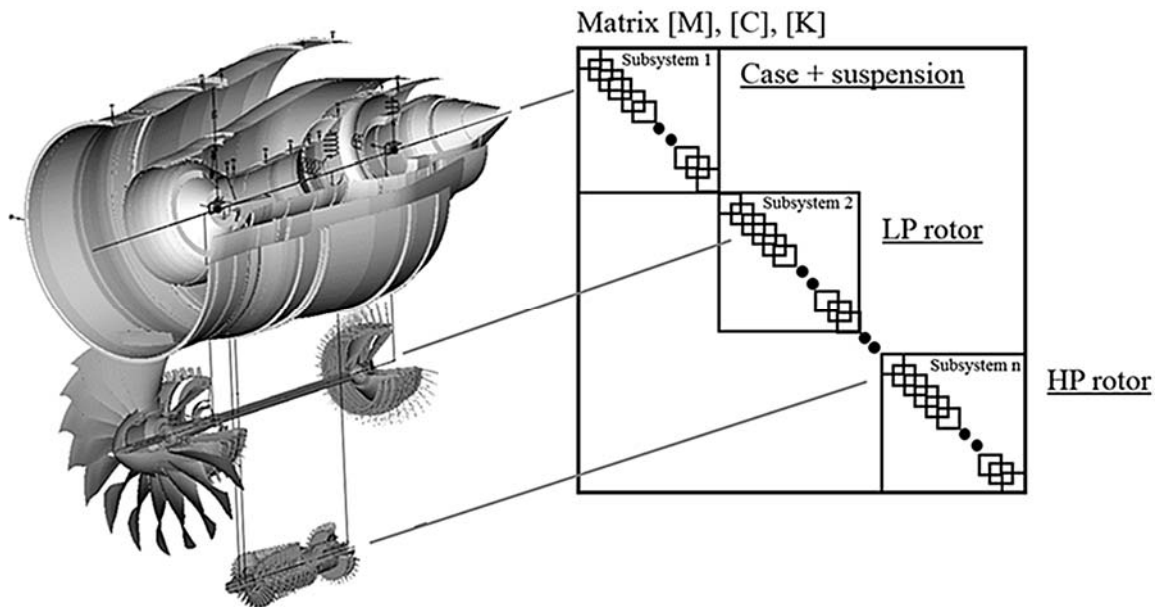


Fig. 1.

The finite element model was formed with usage of two-node finite elements—beams and shells. The model was structured in form of engine main subsystems, which are its rotors, case, and suspension mounts. Damping of engine struts was taken into account using nondimensional relative damping coefficient $\xi = 0.1$ [17]. Damping coefficients for all dampers of the engine were assumed to be constant and equal to $C_{xx} = C_{yy} = 10^5$ N s/m.

Mathematical description of each subsystem is given by their corresponding mass and inertia, stiffness and damping matrices, which form joint matrices for the entire dynamic system. Then the general equation of motion of the full engine dynamic system was formed, which in short form for the linear dynamic system can be written as an expression:

$$\mathbf{M}\ddot{\mathbf{q}} + \mathbf{C}\dot{\mathbf{q}} + \mathbf{K}\mathbf{q} = \mathbf{Q}, \quad (1)$$

where \mathbf{M} is the mass and inertia matrix; \mathbf{C} is the damping and gyroscopic matrix; \mathbf{K} is the stiffness matrix; \mathbf{Q} is the matrix of external forces; \mathbf{q} is the displacement vector.

Solution of the left-hand part of the general equation of motion for dynamic system of the engine allows obtaining a variety of natural frequencies of dynamic systems in the specified calculation range, where critical speeds correspond to intersections of natural frequency lines for various modes with excitation lines related to speeds of engine rotors. Working principles of calculation algorithms, used in DYNAMICS R4 for solution of dynamic systems equations of motion, were described in detail in papers [18, 19].

TYPES OF AIRCRAFT ENGINE RESONANT MODES

Resonant modes, which may appear in the operating range of rotors of aircraft engine dynamic system model, can be conventionally classified by their mode shapes on the three general groups: rotor modes, case modes, and coupled modes. Each resonant mode can be further classified as axial, torsional, or lateral vibration. Main types of resonant modes of a “rotor–case–suspension” dynamic system in the lateral direction in terms of the aircraft engine model examined in this paper are shown in Fig. 2. Here (a)—the rotor mode; (b)—the case mode; (c)—the coupled mode (rotor–case–suspension). Further, the term critical speeds will be used for description of aircraft engine model vibrations in lateral direction only.

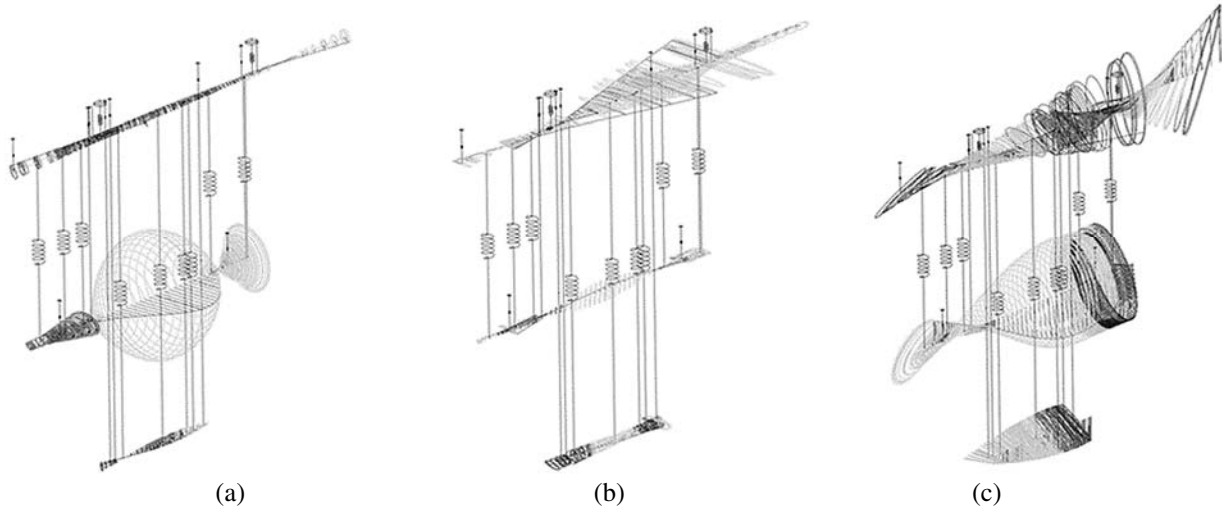


Fig. 2.

When aircraft engine dynamic system is subjected to rotor vibration modes, the largest deformations will be inherent to structural elements of its rotors, while for the case vibration modes—to structural elements of its cases. For coupled modes, it is common to have significant deformations of both rotor and case structural elements. The most dangerous resonant modes are rotor and coupled modes, since the aircraft engine dynamic system always has excitation source for them in the form of residual unbalances of its rotors. If rotor does not have a sufficient separation margin from operating modes

related to its bending mode, then unbalances distributed along rotor body may cause significant rotor deflections leading not only to large engine vibrations, but also to significant stresses in rotor structural elements. Appearance of case resonant modes can be caused by existence of case natural frequencies in the operating range of the engine, where the rotor is also the main excitation source. At the same time, the presence of a large number of joint elements in the aircraft engine case structure and the structural damping implemented in its joints along with the usage of engine elastic-damper supports may lead to situation that the case resonant modes either are not excited at all due to rotor vibrations damping realized in its damper supports, or excited, but with vibration amplitudes being significantly smaller than amplitudes of the rotor modes due to the existence of sufficient damping in aircraft engine dynamic system.

Coupled “rotor–case–suspension” modes are more complex and difficult to predict (e.g., when models of the engine rotor group are observed on equivalent supports), since their critical speeds and mode shapes may significantly differ from the critical speeds and mode shapes of separate rotors or engine case modes [20]. The main excitation sources for coupled lateral modes of “rotor–case–suspension” system are also residual unbalances of the engine rotors. Existence of different rotors operating at various speeds inside the aircraft engine, which are not mechanically bonded with each other, creates a complex excitation nature, which also should be taken into account when analyzing dynamic systems such as “rotor–case–suspension” systems.

For the correct engine mode shape classification, it is necessary to analyze each mode evaluating mode shapes for engine main subsystems, distinguishing subsystems with obvious significant deformations. It should be noted that the observed classification of lateral mode shapes is conventional, since even for pronounced rotor modes, small deformations will be still observed at engine cases, while for pronounced case modes in contrast—at its rotors. When selecting sensor locations in aircraft engine, it is necessary to take into account the nature of its main mode shapes, which are planned to be identified during experimental measurements. Each individual mode shape is differed by position and number of its node and antinode points [21]. Antinode points are the points, where mode shapes amplitudes reach their maximum values, while node points are the points, where vibration amplitudes turn to zero. In order to be able to efficiently identify each specific aircraft engine resonant mode, the installed sensor should be distant from the node points of corresponding mode shape. At the same time, location of the sensor close to mode shape node point (together with sensors installed at antinode points) also possess high information assessment, since it allows us to verify mode shape by position of its node points. However, this approach requires a large number of sensors installed in the aircraft engine.

The spatial nature of aircraft engine suspension mounts on the pylon and the presence of clearances in its bearings and dampers leads to appearance of orthotropy for dynamic system elastic properties in orthogonal direction, which in turn influences on the orbits of individual model element sections, transforming them to a pronounced elliptical shape. Engine aggregates, installed on its cases, may also affect the emergence of orthotropy in engine dynamic system. Orthotropy presence in the dynamic system leads to the necessity to account and control not only direct precession “rotor–case–suspension” system mode shapes, but also backward precession mode shapes. In such systems appearance of mixed precession mode shapes is also possible, where one part of the rotor is subjected to direct precession, while the other—to backward one [22]. Existence of the dynamic systems orthotropy may also significantly influence the sensors information assessment, when they are installed in orthogonal direction.

For the aircraft engine model examined in this paper, a critical speed mode shape analysis was performed, where excitation of critical speeds by the engine low pressure (LP) (Fig. 3a) and high pressure (HP) (Fig. 3b) rotors was observed in the range of rotor speeds two times higher than engine maximum operating speed mode.

Analysis of the results showed, that 50–58% of the critical speed mode shapes obtained by calculation were identified as coupled “rotor–case–suspension” modes, 11–13% were case modes, while the others were related with rotor modes.

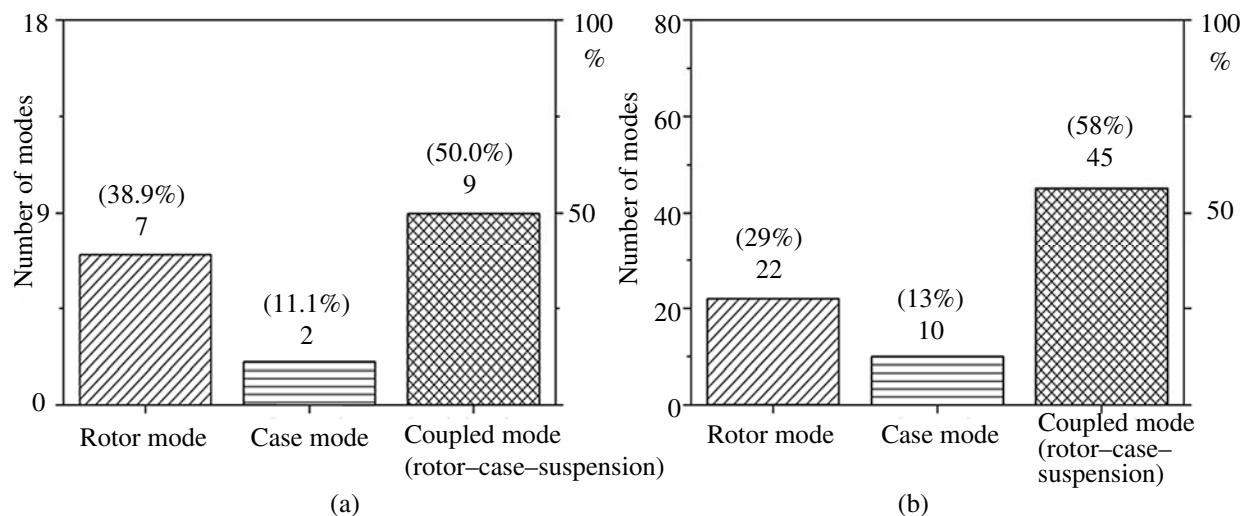


Fig. 3.

METHOD FOR SENSOR LOCATION SELECTION

In stationary gas turbomachinery, it is common to place vibration sensors at bearing housings, since they actively respond to the main dynamic forces, occurring during engine operation, and their level of vibration reflects the general vibrational state of the machine. Selection of the measuring points for the stationary ground gas turbine units is regulated by relevant standards, e.g., Standard [23]. In aircraft engine, such uniform standards do not exist due to individual features of each engine. Installation of sensors in vicinity of aircraft engine bearing housings is associated with significant technical difficulties, due to their inaccessibility, influence of high temperature and actual lack of sufficient free space for sensors installation. Thus, vibration sensors in aircraft engine are usually set at suspension mounts or near them. When aircraft engine is equipped with vibration sensors for identification of its critical speeds and their associated mode shapes, it is common to install additional sensors on available flange joints of its cases. Installation of sensors at cases flange joints allows avoiding the case shell vibration modes, which may significantly complicate identification of the engine main resonant modes in lateral direction.

The initial information assessment for vibration sensor locations can be performed based on analysis of critical speed mode shapes results obtained by simulation for aircraft engine model (Fig. 4).

For this purpose, first, it is necessary to prepare model of aircraft engine and set up all elements of the model on thermal state corresponding to expected temperatures of the engine at its operating mode. Then, it is required to set up the places of virtual sensor locations in the model, where information assessment to control critical speeds of the engine will be evaluated during the analysis. The next step is to select the excitation source in model (LP/IP/HP rotor) and determine the frequency range for simulation. Further, calculation of natural frequencies of the aircraft engine model without damping and rotation is performed, followed by calculation of model critical speeds including effects of damping and rotor rotation. Thereafter, recording of N lateral critical speed mode shapes, selected from all critical speed mode shapes (axial, lateral, torsional) obtained from simulation, is carried out.

After selection of mode shapes related with lateral critical speeds, their analysis and sensor locations information assessment tables development are performed. Each mode shape is preliminary analyzed and classified based on mode shape type (rotor mode, case mode, coupled mode). Nodal and antinode points are determined for each mode shape. Recording of vibration vector projections of aircraft engine model elements in vertical and horizontal directions (U_x , U_y) at places, where virtual sensors for each of the selected N mode shapes is further implemented as

$$U_{ix} = \text{Re}(U_{ix}) + \text{Im}(U_{ix})i; \tag{2}$$

$$U_{iy} = \text{Re}(U_{iy}) + \text{Im}(U_{iy})i. \tag{3}$$

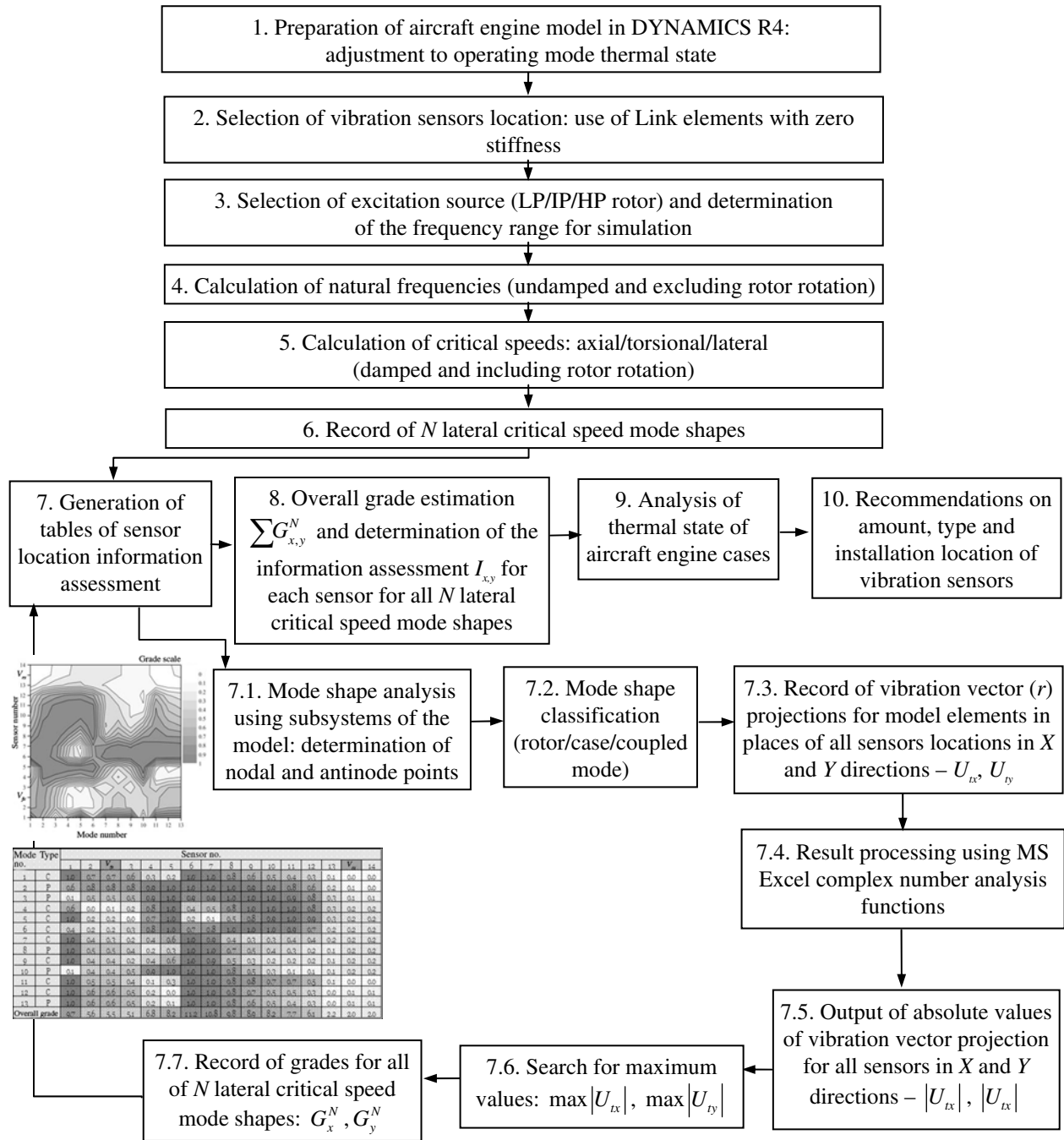


Fig. 4.

Since vector projections output in DYNAMICS R4 in complex numbers, further, the results obtained are processed using the complex number analysis and absolute values of vector projections for model elements $|U_{ix}|, |U_{iy}|$ for each of the selected N critical speed mode shapes are implemented as

$$|U_{ix}| = \sqrt{(\operatorname{Re}(U_{ix}))^2 + (\operatorname{Im}(U_{ix}))^2}; \quad (4)$$

$$|U_{iy}| = \sqrt{(\operatorname{Re}(U_{iy}))^2 + (\operatorname{Im}(U_{iy}))^2}. \quad (5)$$

Then search for the maximum values $\max|U_{ix}|$ and $\max|U_{iy}|$ of model elements vibration vector at places of sensors locations is realized. Next, grades G_x^N , G_y^N for each sensor for each of the selected N critical speed mode shape are calculated, forming the tables of information assessment for sensor locations. Sensors are evaluated in groups by subsystems, in which they are installed in the model. The grade represents the ratio of absolute vibration vector projection of model element in place, where the sensor is installed, to the maximum value of vibration vector projections defined for a group of sensors, which includes this sensor:

$$G_x^N = \frac{|U_{ix}|}{\max|U_{ix}|}; \quad (6)$$

$$G_y^N = \frac{|U_{iy}|}{\max|U_{iy}|}. \quad (7)$$

Assessment criteria are the follows: 1—the best value, 0—the worst value:

$$0 \ll G_x^N; \quad G_y^N \ll 1. \quad (8)$$

Table cells in all tables are highlighted with colors set in accordance with the proposed assessment criteria. For each table of information assessment for vibration sensors installed in horizontal and vertical directions, contour color plots are also built with color distribution set in compliance with the assessment criteria. When creation of tables is completed, a count of overall grade for each sensor is performed. Overall grade for each sensor is formed as a sum of its grades for each of the observed N critical speed mode shapes:

$$\sum G_{x,y}^N = G_{x,y}^1 + G_{x,y}^2 + \dots + G_{x,y}^N. \quad (9)$$

Information assessment for each sensor is determined in percentage as a ratio of overall sensor grade to a number of N critical speed mode shapes considered:

$$I_{x,y} = \frac{\sum G_{x,y}^N}{N} 100 \%. \quad (10)$$

In order to select the vibration sensor type (general usage/high temperature) to include in the vibration sensor scheme developed for the engine, it is necessary to perform the thermal state analysis of the aircraft engine cases. Such analysis is highly important during development of the scheme of the aircraft engine vibration sensors layout, since working environment temperature increase may significantly influence the sensitivity change of accelerometer sensor operating in such environment.

EVALUATION OF SENSOR LOCATION INFORMATION ASSESSMENT

For a model of high-bypass turbofan engine, 14 sections were selected on cases of its flange joints related to its main load frame structure, where vibration sensor installation is possible. Figure 5 demonstrates the spatial position of the sensors on the outer (Fig. 5a) and inner (Fig. 5b) cases in 3D

visualization of the engine model. The sensors were oriented in the horizontal and vertical directions. Permanent sensors (V_{β} , V_{rs}) were installed on suspension joints of the engine model.

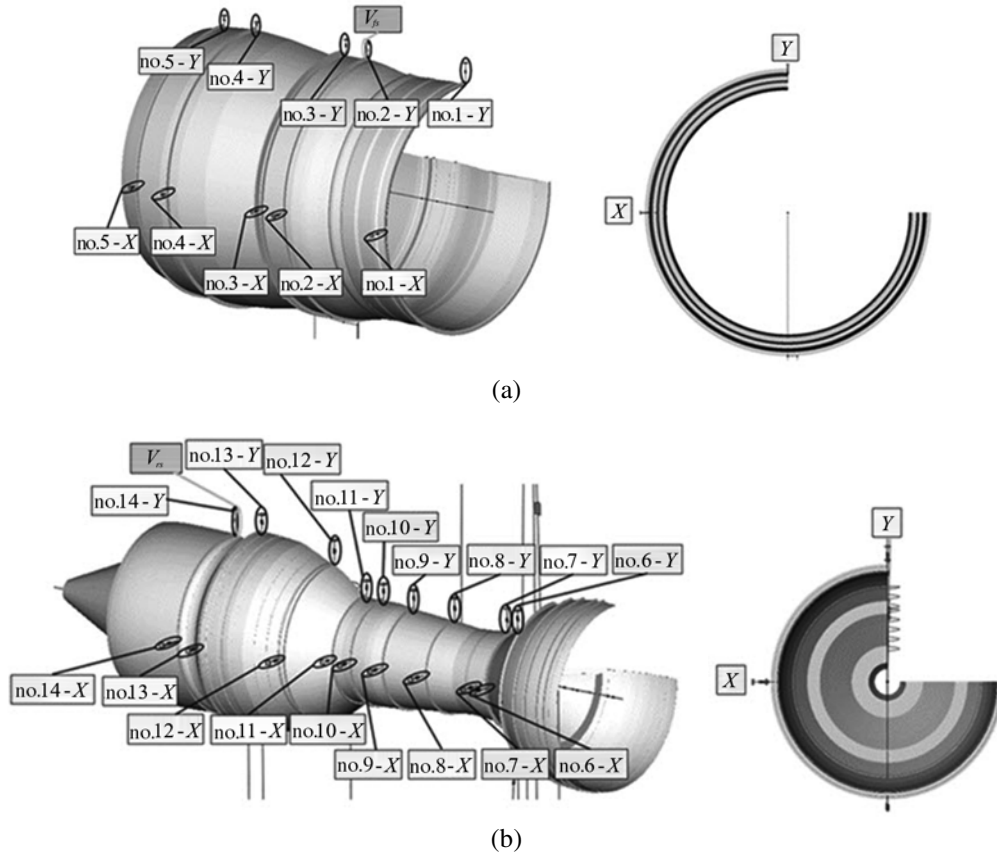


Fig. 5.

Information assessment for vibration sensors installed in the model was evaluated based on the proposed method for critical speeds falling in the operating range of its LP and HP rotors. Tables of information assessment for vibration sensor locations obtained based on simulation results are shown in Fig. 6, where the mode shape types are designated as follows: R—rotor mode, C—case resonance; RCS—couple mode (rotor–case–suspension). The lines highlight the operating modes of the engine: ground idle mode (IDLE) and maximum operating mode (MAX).

Vibration control in X direction															Vibration control in Y direction														
Mode No	Type	Sensor No																											
		1	2	V_{β}	3	4	5	6	7	8	9	10	11	12	13	V_{rs}	14												
1	RCS	1.0	0.7	0.7	0.6	0.3	0.2	1.0	1.0	0.8	0.6	0.5	0.4	0.3	0.1	0.0	0.0	IDLE											
2	R	0.6	0.8	0.8	0.8	0.5	1.0	1.0	1.0	1.0	0.9	0.9	0.8	0.6	0.2	0.1	0.0												
3	R	0.1	0.5	0.5	0.5	0.9	1.0	0.9	0.9	1.0	1.0	1.0	0.9	0.8	0.3	0.1	0.1												
4	RCS	0.6	0.0	0.1	0.2	0.8	1.0	0.4	0.5	0.8	1.0	1.0	1.0	0.8	0.3	0.2	0.2												
5	RCS	1.0	0.2	0.2	0.0	0.7	1.0	0.2	0.1	0.5	0.8	0.9	1.0	0.9	0.3	0.2	0.2												
6	RCS	0.4	0.2	0.2	0.3	0.8	1.0	0.7	0.8	1.0	1.0	1.0	0.9	0.7	0.2	0.2	0.2												
7	RCS	1.0	0.4	0.3	0.2	0.4	0.6	1.0	0.9	0.4	0.3	0.3	0.4	0.4	0.2	0.2	0.2												
8	R	1.0	0.5	0.5	0.4	0.2	0.3	1.0	1.0	0.7	0.5	0.4	0.3	0.2	0.1	0.2	0.2												
9	RCS	1.0	0.4	0.4	0.2	0.4	0.6	1.0	0.9	0.5	0.3	0.2	0.2	0.2	0.1	0.2	0.2												
10	R	0.1	0.4	0.4	0.5	0.9	1.0	1.0	1.0	0.8	0.5	0.3	0.1	0.1	0.1	0.2	0.2	MAX											
11	RCS	1.0	0.5	0.5	0.4	0.1	0.3	1.0	1.0	0.8	0.8	0.7	0.7	0.5	0.1	0.0	0.0												
12	RCS	1.0	0.6	0.6	0.5	0.2	0.0	1.0	1.0	0.8	0.7	0.5	0.5	0.3	0.0	0.1	0.1												
13	RCS	1.0	0.6	0.6	0.5	0.2	0.1	1.0	1.0	0.8	0.6	0.5	0.4	0.3	0.0	0.1	0.1												
Overall grade		9.7	5.6	5.5	5.1	6.8	8.2	11.2	10.8	9.8	8.9	8.2	7.7	6.1	2.2	2.0	2.0												

Vibration control in X direction															Vibration control in Y direction														
Mode No	Type	Sensor No																											
		1	2	V_{β}	3	4	5	6	7	8	9	10	11	12	13	V_{rs}	14												
1	RCS	1.0	0.0	0.0	0.0	1.0	1.0	0.0	0.0	0.0	0.0	0.0	0.0	0.0	0.0	0.0	0.0	IDLE											
2	R	1.0	0.2	0.2	0.1	0.6	0.9	0.5	0.3	0.5	0.8	0.9	1.0	0.9	0.4	0.4	0.4												
3	R	1.0	0.3	0.3	0.1	0.5	0.8	1.0	0.8	0.0	0.4	0.6	0.7	0.7	0.6	0.6	0.6												
4	RCS	1.0	0.2	0.2	0.1	0.6	0.9	1.0	0.7	0.2	0.7	0.9	1.0	1.0	0.7	0.8	0.8												
5	RCS	1.0	0.2	0.2	0.0	0.7	1.0	0.2	0.2	0.0	0.7	0.9	0.8	0.6	0.2	0.5	0.6	0.7											
6	RCS	1.0	0.2	0.2	0.0	0.7	1.0	0.5	0.3	0.5	0.8	0.9	1.0	1.0	0.7	0.8	0.8												
7	RCS	0.5	0.1	0.1	0.2	0.8	1.0	0.5	0.5	0.8	0.9	1.0	1.0	0.8	0.1	0.1	0.1												
8	R	0.7	0.2	0.2	0.2	0.8	1.0	0.5	0.5	0.8	0.9	1.0	1.0	0.8	0.5	0.5	0.5												
9	RCS	0.7	0.0	0.0	0.1	0.8	1.0	0.4	0.5	0.8	1.0	1.0	1.0	0.9	0.4	0.4	0.4												
10	R	0.4	0.4	0.2	0.3	0.8	1.0	1.0	1.0	0.9	0.7	0.6	0.5	0.3	0.2	0.2	0.2	MAX											
11	RCS	1.0	0.4	0.4	0.3	0.2	0.4	1.0	1.0	1.0	1.0	1.0	1.0	1.0	0.9	0.5	0.5												
12	RCS	1.0	0.9	0.9	0.9	1.0	1.0	1.0	1.0	0.7	0.4	0.3	0.2	0.1	0.1	0.1	0.1												
13	RCS	0.8	0.8	0.8	0.8	1.0	1.0	1.0	1.0	0.9	0.8	0.6	0.6	0.4	0.1	0.2	0.2												
Overall grade		11.1	3.9	3.8	3.2	9.5	11.9	9.2	8.3	7.3	8.9	9.5	9.5	8.5	5.1	5.5	5.6												

Mode type: R – Rotor mode; C – Case mode; RCS – Coupled mode (rotor-case-suspension)

(a)

Fig. 6.

Vibration control in X direction															Vibration control in Y direction																				
Mode No	Type	Sensor No													V _{fs}	Mode No	Type	Sensor No													V _{fs}				
		1	2	3	4	5	6	7	8	9	10	11	12	13				1	2	3	4	5	6	7	8	9	10	11	12	13					
1	RCS	0.0	0.0	0.0	0.0	0.0	0.0	0.0	0.0	0.0	0.0	0.0	0.0	0.0	1	RCS	0.0	0.0	0.0	0.0	0.0	0.0	0.0	0.0	0.0	0.0	0.0	0.0	1						
2	RCS	0.3	0.1	0.4	0.4	0.9	1.0	0.6	0.8	1.0	1.0	0.9	0.9	0.7	0.1	2	RCS	0.0	0.1	0.2	0.1	0.0	0.0	0.0	0.0	0.0	0.0	0.0	0.0	2					
3	RCS	0.4	0.2	0.2	0.3	0.8	1.0	0.4	0.7	0.9	1.0	1.0	0.8	0.3	0.2	3	RCS	1.0	0.2	0.2	0.1	0.8	0.2	0.9	0.7	0.3	0.7	0.9	1.0	1.0	0.6	0.7	0.7		
4	RCS	0.8	0.1	0.1	0.1	0.8	1.0	0.1	0.2	0.7	0.9	1.0	1.0	0.8	0.3	0.2	4	RCS	1.0	0.3	0.3	0.1	0.6	0.3	1.0	0.9	0.4	0.1	0.1	0.1	0.7	0.5	0.7	0.7	
5	R	0.7	0.2	0.2	0.2	0.8	1.0	0.0	0.0	0.9	1.0	1.0	1.0	0.8	0.4	0.4	5	R	1.0	0.2	0.2	0.1	0.7	0.9	1.0	1.0	0.4	0.9	0.9	1.0	0.6	0.4	0.4		
6	R	1.0	0.7	0.2	0.1	1.0	0.2	0.1	0.0	0.0	1.0	1.0	1.0	0.9	0.1	0.2	6	R	1.0	0.9	0.9	0.1	0.4	0.4	1.0	0.9	0.5	0.4	0.3	0.2	0.4	0.6	0.5		
7	RCS	1.0	0.7	0.3	0.2	0.4	0.7	1.0	0.2	0.1	0.3	0.4	0.4	0.2	0.2	0.2	7	RCS	1.0	0.4	0.4	0.3	0.2	0.4	0.8	0.7	0.8	1.0	1.0	1.0	0.7	0.2	0.4	0.4	
8	RCS	1.0	0.4	0.3	0.2	0.4	0.6	1.0	0.9	0.4	0.6	0.1	0.2	0.2	0.1	0.2	8	RCS	0.3	0.2	0.2	0.3	0.1	1.0	0.5	0.4	0.3	0.9	1.0	1.0	0.7	0.1	0.2	0.3	
9	RCS	0.0	0.4	0.2	0.2	0.4	0.6	1.0	0.9	0.4	0.6	0.1	0.2	0.2	0.1	0.2	9	RCS	0.0	0.1	0.1	0.1	1.0	0.4	0.4	0.4	1.0	1.0	1.0	1.0	0.4	0.3	0.3		
10	R	1.0	0.3	0.3	0.2	0.2	0.3	1.0	0.5	0.5	0.0	0.2	0.5	0.5	0.0	0.0	10	R	0.5	0.3	0.3	0.2	0.3	1.0	0.5	0.5	0.9	1.0	1.0	0.8	0.5	0.5	0.5		
11	R	0.0	0.4	0.4	0.5	0.9	1.0	1.0	1.0	0.8	0.4	0.3	0.1	0.1	0.1	0.2	11	R	0.5	0.0	0.2	0.2	0.8	1.0	1.0	1.0	1.0	1.0	0.0	0.0	0.0	0.0	0.0		
12	RCS	1.0	0.4	0.2	0.2	0.6	0.8	0.5	0.5	0.5	1.0	1.0	1.0	0.5	0.5	0.5	12	RCS	1.0	0.4	0.4	0.3	0.2	0.4	1.0	1.0	1.0	1.0	1.0	1.0	0.4	0.5	0.5	0.5	
13	RCS	1.0	0.5	0.4	0.3	0.2	0.1	1.0	1.0	1.0	1.0	1.0	1.0	0.0	0.0	0.0	13	RCS	1.0	0.4	0.4	0.3	0.2	0.4	1.0	1.0	1.0	1.0	1.0	1.0	0.4	0.5	0.5	0.5	
14	RCS	1.0	0.6	0.6	0.5	0.2	0.1	1.0	1.0	0.9	0.7	0.5	0.5	0.0	0.0	0.0	14	RCS	1.0	0.7	0.7	0.7	0.4	0.5	1.0	1.0	0.8	0.6	0.4	0.3	0.2	0.1	0.1	0.1	
15	R	1.0	0.5	0.5	0.4	0.1	0.3	0.6	0.6	0.8	0.9	1.0	1.0	0.9	0.3	0.2	15	R	1.0	0.4	0.5	0.4	0.2	0.4	0.8	0.8	1.0	1.0	1.0	0.9	0.7	0.3	0.2	0.2	
16	RCS	0.3	0.1	0.1	0.2	0.8	1.0	0.1	0.1	0.4	0.7	0.9	1.0	0.9	0.4	0.4	16	RCS	1.0	0.3	0.3	0.1	0.7	1.0	0.3	0.4	0.4	0.9	1.0	1.0	0.9	0.4	0.4	0.4	
17	RCS	0.3	0.2	0.2	0.2	0.8	1.0	0.1	0.1	0.4	0.7	0.9	1.0	0.9	0.4	0.4	17	RCS	1.0	0.4	0.4	0.3	0.6	0.9	0.5	0.6	0.7	0.9	1.0	0.9	0.7	0.8	0.8		
18	RCS	0.4	0.2	0.2	0.2	0.8	1.0	0.1	0.1	0.4	0.7	0.9	1.0	0.9	0.4	0.4	18	RCS	1.0	0.4	0.4	0.3	0.6	0.9	0.5	0.6	0.7	0.9	1.0	0.9	0.5	0.5	0.5		
19	RCS	0.2	0.2	0.2	0.2	0.8	1.0	0.1	0.1	0.4	0.7	0.9	1.0	0.9	0.4	0.4	19	RCS	0.7	0.4	0.4	0.3	0.8	1.0	0.5	0.5	0.4	0.7	0.9	1.0	0.6	0.5	0.6		
20	RCS	0.4	0.2	0.2	0.2	0.8	1.0	0.1	0.1	0.4	0.7	0.9	1.0	0.9	0.4	0.4	20	RCS	0.7	0.4	0.4	0.4	0.9	1.0	0.7	0.7	0.5	0.7	0.9	1.0	0.5	0.4	0.4		
21	RCS	1.0	0.4	0.4	0.2	0.2	0.3	1.0	0.0	0.3	0.7	0.9	1.0	1.0	0.7	0.7	21	RCS	1.0	0.4	0.4	0.2	0.6	0.9	0.1	0.0	0.3	0.7	0.9	1.0	0.6	0.6	0.6		
22	R	1.0	0.5	0.5	0.4	0.0	0.1	0.1	0.3	0.7	0.9	1.0	1.0	0.8	0.8	0.9	22	R	1.0	0.6	0.6	0.5	0.7	0.8	0.1	0.1	0.4	0.7	0.9	1.0	0.6	0.5	0.5		
23	RCS	1.0	0.9	0.4	0.4	0.1	0.2	0.2	0.1	0.4	0.6	0.9	1.0	0.9	0.9	0.9	23	RCS	1.0	0.7	0.4	0.4	0.2	0.2	0.1	0.0	0.3	0.7	0.9	1.0	0.6	0.4	0.4		
24	R	1.0	0.5	0.5	0.4	0.1	0.2	0.1	0.1	0.3	0.7	0.9	1.0	0.9	0.9	0.9	24	R	1.0	0.6	0.6	0.6	0.6	0.6	0.2	0.2	0.3	0.7	0.9	1.0	0.6	0.6	0.6		
25	C	1.0	0.5	0.5	0.4	0.1	0.0	0.0	0.1	0.4	0.6	0.6	0.6	0.3	0.7	1.0	25	C	1.0	0.0	0.0	0.0	0.0	0.0	0.0	0.0	0.0	0.0	0.0	0.0	0.0	0.0	0.0		
26	RCS	0.9	0.6	0.6	0.4	0.2	0.2	0.4	0.6	1.0	0.8	0.9	0.8	0.1	0.4	0.4	26	RCS	1.0	0.6	0.5	0.4	0.4	0.5	0.1	0.1	0.4	0.9	1.0	0.9	0.6	0.5	0.5		
27	C	0.0	0.0	0.0	0.0	0.0	0.0	0.0	0.0	0.0	1.0	1.0	1.0	1.0	0.0	0.0	27	C	1.0	0.0	0.0	0.0	0.0	0.0	0.1	0.2	0.4	0.9	1.0	1.0	0.7	0.4	0.6	0.6	
28	RCS	1.0	0.4	0.4	0.3	0.3	0.9	1.0	1.0	0.4	0.5	0.3	0.5	0.7	0.6	0.6	28	RCS	1.0	0.4	0.4	0.4	0.4	0.4	0.0	0.0	0.5	1.0	0.7	0.7	0.7	1.0	1.0		
29	RCS	1.0	0.4	0.4	0.3	0.3	0.9	1.0	1.0	0.4	0.5	0.3	0.5	0.7	0.6	0.6	29	RCS	1.0	0.4	0.4	0.3	0.6	0.7	0.1	0.1	0.2	0.3	0.4	0.4	0.4	0.8	1.0	1.0	
30	R	1.0	0.4	0.4	0.3	0.3	0.9	1.0	1.0	0.4	0.5	0.4	0.3	0.0	0.0	1.0	30	R	1.0	0.4	0.4	0.3	0.3	0.3	0.1	0.1	0.6	1.0	1.0	1.0	0.7	0.4	0.6	0.6	
31	R	1.0	0.4	0.2	0.2	0.4	0.4	0.1	0.2	0.4	0.4	0.4	0.4	0.0	0.0	1.0	31	R	1.0	0.4	0.4	0.3	0.4	0.2	0.1	0.1	0.6	0.9	1.0	1.0	0.7	0.4	0.6	0.6	
32	C	0.0	0.0	0.0	0.0	0.0	0.0	0.0	0.0	0.0	0.0	0.0	0.0	0.0	0.0	0.0	32	C	0.0	0.0	0.0	0.0	0.0	0.0	0.0	0.0	0.0	0.0	0.0	0.0	0.0	0.0	0.0	0.0	
33	C	0.0	0.0	0.0	0.0	0.0	0.0	0.0	0.0	0.0	0.0	0.0	0.0	0.0	0.0	0.0	33	C	1.0	0.0	0.0	0.0	1.0	1.0	0.4	0.4	0.6	1.0	0.6	0.4	0.0	1.0	1.0	1.0	
34	R	1.0	0.4	0.3	0.2	0.4	0.4	0.2	0.3	0.4	0.4	0.3	0.1	0.2	0.3	1.0	34	R	1.0	0.4	0.3	0.2	0.4	0.4	1.0	1.0	0.7	0.2	0.3	0.4	0.6	0.4	0.4	0.4	
35	C	0.0	0.0	0.0	0.0	0.0	0.0	0.0	0.0	0.0	0.0	0.0	0.0	0.0	0.0	0.0	35	C	0.0	0.0	0.0	0.0	0.0	0.0	0.0	0.0	0.0	0.0	0.0	0.0	0.0	0.0	0.0	0.0	0.0
36	R	1.0	0.4	0.4	0.3	0.4	0.3	0.1	0.1	0.5	1.0	1.0	0.9	0.6	0.1	0.7	36	R	1.0	0.3	0.3	0.2	0.4	0.4	0.4	0.4	0.4	0.5	0.7	0.9	1.0	1.0	1.0	1.0	
37	RCS	1.0	0.3	0.3	0.2	0.4	0.4	0.4	0.4	0.1	0.3	0.5	0.6	0.2	0.7	1.0	37	RCS	1.0	0.3	0.3	0.2	0.4	0.5	1.0	1.0	0.9	0.4	0.1	0.3	0.6	0.7	0.7	0.7	
38	C	0.0	0.0	0.0	0.0	0.0	0.0	0.0	0.0	0.0	0.0	0.0	0.0	0.0	0.0	0.0	38	C	0.0	0.0	0.0	0.0	0.0	0.0	0.0	0.0	0.0	0.0	0.0	0.0	0.0	0.0	0.0	0.0	0.0
39	RCS	1.0	0.2	0.2	0.1	0.4	0.4	1.0	1.0	0.0	0.2	0.4	0.6	0.5	0.6	0.7	39	RCS	1.0	0.2	0.1	0.1	0.6	0.6	0.5	0.5	0.8	0.6	0.3	0.1	0.8	1.0	1.0	1.0	
40	RCS	1.0	0.1	0.1	0.0	0.4	0.4	1.0	1.0	0.7	0.1	0.3	0.4	0.3	0.5	0.5	40	RCS	1.0	0.2	0.1	0.1	0.6	0.6	0.8	0.6	0.8	0.6	0.3	0.1	0.8	1.0	1.0	1.0	
41	RCS	1.0	0.1	0.1	0.0	0.4	0.4	1.0	1.0	0.8	0.1	0.4	0.6	0.7	0.3	0.5	41	RCS	1.0	0.1	0.1	0.1	0.6	0.6	0.3	0.4	0.5	0.5	0.4	0.3	0.4	0.9	1.0	1.0	
42	RCS	1.0	0.1	0.1	0.0	0.4	0.4	1.0	1.0	0.8	0.1	0.4	0.6	0.7	0.3	0.5	42	RCS	1.0	0.1	0.1	0.1	0.6	0.6	0.5	0.5	0.1	0.4	0.5	0.2	0.2	0.9	1.0	1.0	
43	RCS	1.0	0.0	0.0	0.0	0.3	0.3	1.0	1.0	0.2	0.7	0.3	0.7	0.5	0.2	0.3	43	RCS	1.0	0.0	0.0	0.0	0.5	0.5	0.1	0.1	0.7	0.7	0.5	0.4	0.5	0.4	0.5	0.4	
44	C	1.0	0.1	0.1	0.2	0.4	0.2	0.2	0.0	0.1	0.0	0.4	0.7	0.9	1.0	44	C	1.0	0.0	0.0	0.4	0.4	0.3												

Overall grades G and information assessment I for sensor locations to control critical speeds excited by LP (Fig. 9a) and HP (Fig. 9b) rotors in the observed aircraft engine model are as follows.

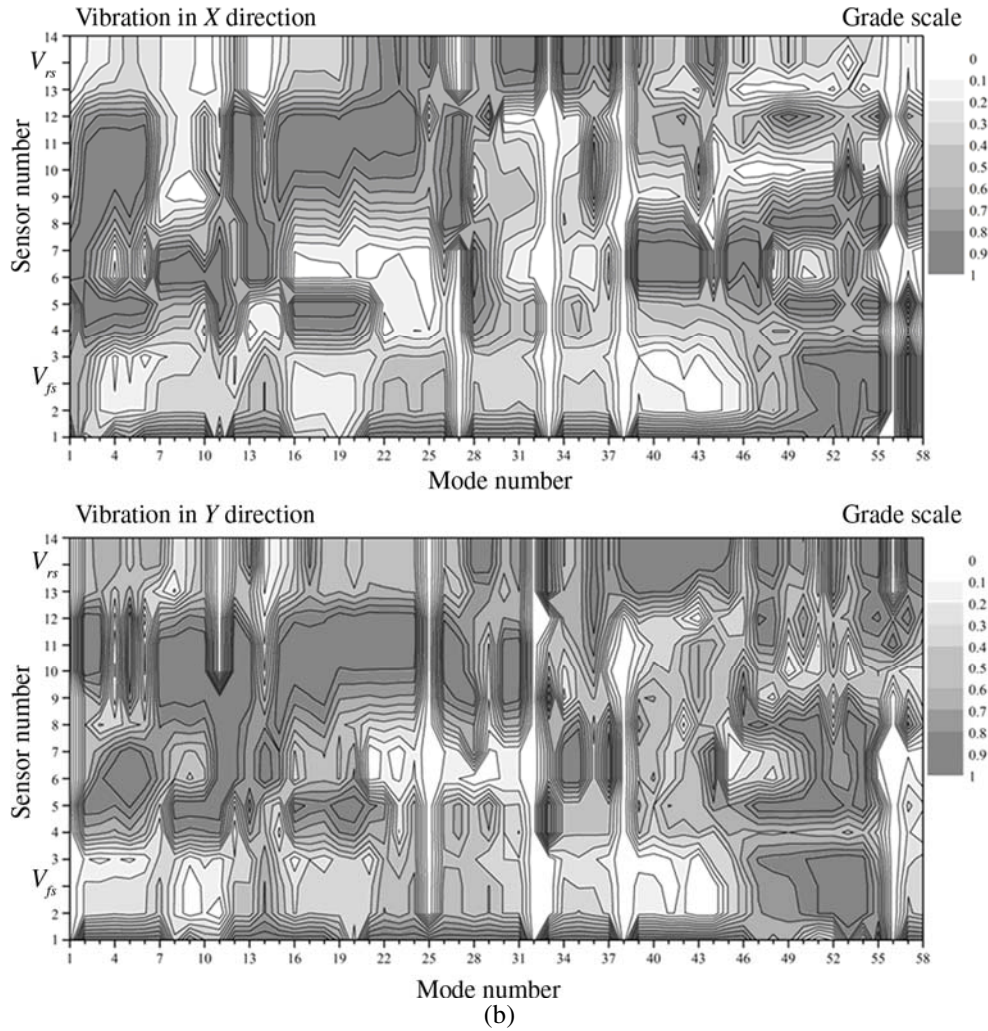


Fig. 8.

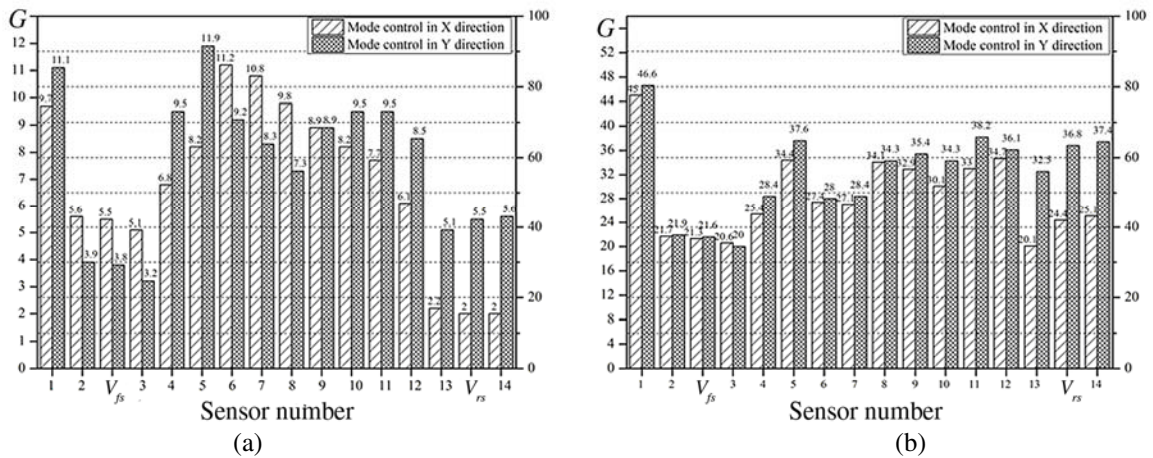


Fig. 9.

Simulation results obtained for aircraft engine model revealed that for the model verification based on the data of experimental measurements in order to get maximum information about critical speeds of the real aircraft engine, it is recommended to use uniaxial sensors for vibration control in the X and Y directions installed at brackets attached to flange joints of outer case in planes nos. 1, 4 and 5 (see Fig. 5a). At the inner case of the engine, it is recommended to use uniaxial sensors to control vibrations in the X and Y directions installed at brackets attached to flange joints in planes nos. 6–12 (see Fig. 5b).

It should be noted that calculations performed are evaluative, since they reflect excitation of all possible critical speeds for dynamic system of an aircraft engine, while at the real engine, appearance of specific critical speeds often depends on a certain distribution of residual unbalances. Excitation of some critical speeds may require “exotic” combination of residual unbalances located on rotors of the engine, and thus, such critical speeds may not be excited with standard distribution of unbalances localized on the main assembling units of its rotors. To exclude the latter and reduce the number of critical speeds that need to be controlled with vibration sensors, it is required to perform a series of calculations with various unbalances combinations. It is possible to perform modeling of aircraft engine dynamics similar to its real operation with mutual excitation from unbalance distribution at all rotors of the engine using the algorithms of nonstationary analysis implemented in DYNAMICS R4.

CONCLUSIONS

A method to equip aircraft engine with vibration sensors based on calculation and analysis of critical speed mode shapes obtained for its model was proposed. The method was tested on the model of high-bypass aircraft engine built in software for rotor dynamics simulation—DYNAMICS R4, allowing us to evaluate information assessment of vibration sensor locations installed on the engine cases and further form the scheme of sensors with high information assessment of critical speeds and their shapes of vibration mode of the aircraft engine dynamic system.

REFERENCES

1. *API RP 684. Paragraphs Rotodynamic Tutorial: Lateral Critical Speeds, Unbalance Response, Stability, Train Torsionals and Rotor Balancing*, Washington: American Petroleum Institute, 2005.
2. Zrelov, V.A., Prodanov, M.E., and Belousov, A.I., Analysis of Domestic Aircraft Gas Turbine Engine Development Dynamics, *Izv. Vuz. Av. Tekhnika*, 2008, vol. 51, no. 4, pp. 7–12 [Russian Aeronautics (Engl. Transl.), vol. 51, no. 4, pp. 354–361].
3. *Vibratsii v tekhnike. Spravochnik: v shesti tomakh* (Vibration in Engineering: Handbook, in six vol.), vol. 3: *Kolebaniya mashin, konstruktssii i ikh elementov* (Vibrations of Machines, Structures and Their Elements), Dimentberg, F.M. and Kolesnikov, K.S. Eds., Moscow: Mashinostroenie, 1980.
4. Karasev, V.A., Maksimov, V.P., Sidorenko, M.K., *Vibratsionnaya diagnostika gazoturbinnnykh dvigatelei* (Aircraft Engines Vibration Diagnostics), Moscow: Mashinostroenie, 1978.
5. Natanzon, V.Ya., Influence of Case Vibrations on Rotor Critical Speeds, in *Kolebaniya v turbomashinakh* (Turbomachinery Vibrations), Serensen, S.V., Ed., Moscow: AN SSSR, 1956, pp. 49–56.
6. Krukov, K.A., Rotor-Case Coupled Lateral Vibrations of Aircraft Engine, *Trudy MAI*, 1959, no. 100, pp. 5–59.
7. Gurov, A.F., *Sovmestnye kolebaniya v gazoturbinnnykh dvigatelyakh* (Coupled Vibrations in Gas Turbine Engines), Moscow: Oborongiz, 1962.
8. Khronin, D.V., *Teoriya i raschet kolebanii v dvigatelyakh letatel'nykh apparatov* (Theory and Vibration Simulations in Aircraft Engines), Moscow: Mashinostroenie, 1970.
9. Ivanov, A.V., Calculation of Aircraft Engines Resonance Modes Using Computer Simulations. Vibration and Strength of Aircraft Engines Parts, *Trudy MAI*, 1972, no. 245, pp. 66–76.
10. Lebedev, V.N. and Potapova, O.Yu., Influence of Discrete Friction on Vibration of Gas Turbine Engine, in *Proektirovanie, konstruirovaniye i prochnost' konstruktssii reaktivnykh dvigatelei*: (Design, Construction and Structural Strength of Jet Engines), Moscow: MAI, 1988, pp. 13–16.

11. Chaadaev, K.N. and Novikov, D.K., Dynamics of a Rigid Rotor in the NK-14ST-10 Engine Free Power Turbine with Sliding Bearings, *Izv. Vuz. Av. Tekhnika*, 2009, vol. 52, no. 4, pp. 34–37 [Russian Aeronautics (Engl. Transl.), vol. 52, no. 4, pp. 426–431].
12. Zrellov, V.A., Mironov, A.S., and Prodanov, M.E., Choice of Support Arrangement in Designing Two-Support Rotors of Gas Turbine Engines, *Izv. Vuz. Av. Tekhnika*, 2010, vol. 53, no. 1, pp. 34–36 [Russian Aeronautics (Engl. Transl.), vol. 53, no. 1, pp. 51–56].
13. Nikhamkin, M.Sh., *Vibratsionnye protsessy v gazoturbinnnykh dvigatelyakh* (Vibration Processes in Gas Turbine Engines), Perm: Izd. Perm. Nats. Issled. Politekh. Univ., 2011.
14. Leont'ev, M.K., Davydov, A.V., Degtyarev, S.A., and Gladkii, I.L., To Simulation of Fan Blade out for a High Bypass Ratio Engine, *Izv. Vuz. Av. Tekhnika*, 2014, vol. 57, no. 2, pp. 33–38 [Russian Aeronautics (Engl. Transl.), vol. 57, no. 2, pp. 154–161].
15. Hong, J., Shaposhnikov, K., Zhang, D., and Ma, Y., Theoretical Modeling for a Rotor-Bearing-Foundation System and Its Dynamic Characteristics Analysis, *Proc. of the 9th IFToMM International Conference on Rotor Dynamics, Mechanisms and Machine Science*, 2015, vol. 21, pp. 2199–2214.
16. Leont'ev, M.K., Modal Synthesis in Studying the Dynamic Behavior of Complex Aircraft GTE Systems, *Izv. Vuz. Av. Tekhnika*, 1988, vol. 31, no. 1, pp. 44–48 [Soviet Aeronautics (Engl. Transl.), vol. 31, no. 1, pp. 54–58].
17. Nicholas, J.C., Whalen, J.K., and Franklin, S.D., Improving Critical Speed Calculations Using Flexible Bearing Support FRF Compliance Data, *Proc. of the 15th Turbomachinery Symposium*, USA: Texas A&M University Press, 1986, pp. 69–78.
18. Leont'ev, M.K. and Ivanov, A.V., Modal Analysis of Dynamic Rotor Systems, *Izv. Vuz. Av. Tekhnika*, 2005, vol. 48, no. 3, pp. 31–35 [Russian Aeronautics (Engl. Transl.), vol. 48, no. 3, pp. 45–53].
19. Leont'ev, M.K., Ivanov, A.V., and Degtyarev, S.A., Simulation of Rotor Dynamics Systems with spatial Shaft Position, *Vestnik KGTU im. A.N.Tupoleva*, 2012, no. 2, pp. 231–239.
20. *Dinamika aviatsionnykh gazoturbinnnykh dvigatelei* (Dynamics of Gas Turbine Aircraft Engines), Birger, I.A. and Shorr, B.F., Eds., Moscow: Mashinostroenie, 1981.
21. Babakov, I.M., *Teoriya kolebanii* (Vibration Theory), Moscow: Nauka, 1965.
22. V'yunov, S.A., Gusev, Yu.I., Karpov, A.V., et al., *Konstruktsiya i proektirovanie aviatsionnykh gazoturbinnnykh dvigatelei* (Structure and Design of Aircraft Gas Turbine Engines), Moscow: Mashinostroenie, 1989.
23. GOST R (State Standard) ISO 10816-1-97 *Vibratsiya. Kontrol' sostoyaniya mashiny po rezul'tam izmereniya vibratsii na ne vrashchayushchikhsya chastyakh* (Vibration. Evaluation of Machine Vibration by Measurements on Non-Rotating Parts), Moscow: Izd. Standartov, 1998.